Summary of Previous and Current Research

To find Earth-like planets around Sun-like stars requires digging through unknown, time-varying, and non-stationary instrument and stellar noise. My past research focused on transiting exoplanet data, where I developed transit search algorithms that incorporate complex instrument noise models to improve detection sensitivity to sub-Neptune-sized exoplanets.

Joint Bayesian detection of exoplanet transit signals and structured noise

Conventional transit-detection pipelines perform denoising and detection sequentially, relying on incomplete signal models at each processing step, which can lower overall detection performance, particularly for low radii exoplanets. In **Taaki et al. (2020)**, I developed a detection framework based on joint-modelling of transit signals and Bayesian noise models for correlated instrument noise, as well as time-varying stellar variability. I derive two optimal Neyman-Pearson likelihood ratio detectors; the first marginalizes over the joint-noise model, and the second forms a fixed conditional estimate. The detector uses adaptively estimated priors, to model unknown systematic noise and stellar variability for each target individually. A primary goal of the algorithm is to reduce overfitting; using injection and retrieval tests on unfiltered (SAP) Kepler 30-min light curves, joint-Bayesian detectors showed a relative 3% improvement in detection performance compared to sequential processing for small radius ($\frac{R_P}{R_*} < 0.05$), short-period (< 10 days) exoplanet transit signals, thereby improving the sensitivity to sub-Neptune sized planets around Sun-like stars.

Reproducing exoplanet searches is important for detection pipeline validation and can result in new discoveries. In **Taaki et al. (2025a)**, I developed an end-to-end detection pipeline to search three years of TESS 2-min data from the continuous viewing zone for exoplanets with orbital periods up to 100 days using joint Bayesian detection. Approximately 13% of TESS 2-min data is missing or quality-flagged, the detector was adapted to handle this and refined to improve outlier rejection in post-processing. Because this 2-min light curve data represents a 15 $\times$ increase in data-density as compared to the Kepler 30-min data, I co-authored a successful proposal for a 250K node-hour Blue Waters supercomputing allocation to perform this work. The search achieved a 73% recall rate for TESS Objects-of-Interest present in the data.

Robustly detrending spatially correlated noise in transit light curves

Principle Component Analysis (PCA) is typically applied to fit systematic noise in light curve data, however PCA is known to be prone to overfitting if there are unknown astrophysical signals present such as stellar variability or transits. In **Taaki et al. (2024)**, I develop an algorithm that robustly extracts low-rank instrument systematics from Kepler light curves, enabling astrophysical signals to be cleanly recovered. A modified TV prior is incorporated to regularize the instrument model and encourages correlation among instrument noise estimates for spatially close targets, and allows discontinuities at module boundaries. This constraint is introduced foundationally, such that the full instrumental noise model is solved for based on the spatial correlation prior and jointly for all light curves. Through validation on Kepler light curves, the spatial correlation model is shown to improve the recovery of slow-varying (days) astrophysical signals (such as stellar oscillations and flaring) compared to standard PCA. I maintain an implementation of this method, *spatial-detrend*, on PyPI and Github.

Efficient direct imaging simulations of starshades for HWO

Direct imaging simulations of starshades and other proposed mission concepts are needed to characterize planet detection performance and inform mission design trades. In order to assess the complementary role of a 60 m starshade for NASA's planned Habitable Worlds Observatory (HWO), I develop an optical model of a starshade and perform high-fidelity imaging simulations. Accurate diffractive optical simulations of this form are computationally challenging as both the starshade mask and telescope aperture require extremely fine-scale spatial sampling to control error below the desired 10^{-11} optical contrast level. Simulating this numerically is typically accomplished with zero-padded FFTs, which can have prohibitive run-times. I utilize a Fourier sampling technique, the Bluestein Fast Fourier Transform (B-FFT), to move between varying spatial scales without needing to zero-pad optical fields. This approach obtains a 6× reduction in the computational complexity. The optical core throughput of a direct-imaging system is a key metric that governs exposure time and the potential exoplanetary yield of a mission, and had not previously been precisely quantified for the HWO starshade with realistic segmented or obscured apertures. I use my optical model to evaluate core throughput, incorporating 6 m segmented and obscured telescope apertures, over the visible to near-infrared wavelength band (500-1000 nm), showing close to optimal core throughput of $66-68\%$ within a photometric aperture of radius $0.7\lambda/D$ (**Taaki et al. (2025c)**). I also quantify the Inner Working Angle (IWA, a metric that describes the angular separation from a star at which an exoplanet can be imaged, as $53-58$ mas over the band. Although these IWAs differ by only a few mas, such variations translate into a large gain in accessible phase space, and since planets spend most of their orbit at smaller projected separations than quadrature, this can materially affect observability. Figure 1 shows how our solar system would look, imaged with the HWO starshade concept. I developed these techniques into an open-source Python tool, PyStarshade (**Taaki et al. (2025b)**), offering flexible imaging simulations for a variety of starshade configurations and telescope apertures, as well as the ability to perform tolerancing with imperfect optics.

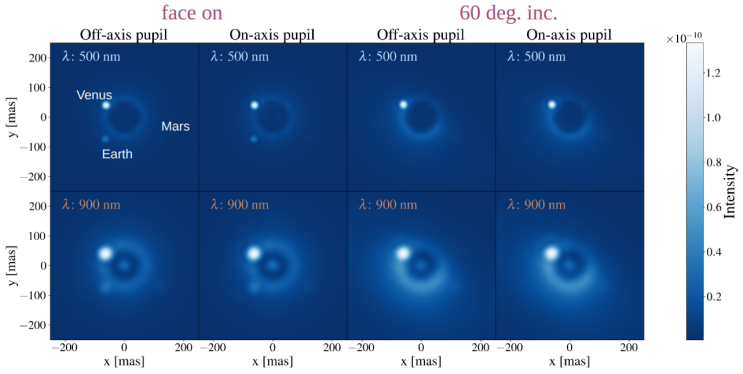

Figure 1: Solar system at 10 pc imaged with the HWO starshade, the system is face-on in columns 1 and 2, and at an inclination of 60 degrees in columns 3 and 4. This scene was simulated with ExoVista, the imaging with PyStarshade. For each inclination, the imaging is simulated for two HWO pupil architectures (unobscured 'off-axis' segmented, and an obscured 'on-axis' segmented pupil). Small planets can be directly imaged in reflected light with the HWO starshade.

Research Proposal: Debiasing Astrometric Starspot Noise to Find and Measure Earth-Mass Exoplanets

Astrometry is a promising technology to both find and measure the masses of terrestrial-sized exoplanets, orbiting in the habitable zones of sun-like stars. Precise mass measurements of these planets are key to characterizing their atmospheric properties and habitability (Damiano et al., 2025), allowing us to identify true Earth-analogs. A limitation of the astrometric technique is stellar jitter noise: as a star rotates, dark starspots, or bright regions of the photosphere may come in and out of view, changing the measured photo-center.

My recent work shows that the astrometric jitter of a rotating star encodes surface-brightness information that can be used to map stellar surfaces. Furthermore, astrometry probes complementary information to light curves, enabling the reconstruction of stellar surfaces that would otherwise be inaccessible. I will use astrometric inversion techniques I am developing to map starspots. By fully modeling starspot induced noise, the minute astrometric signature of an orbiting exoplanet can be clearly identified, bringing us closer to achieving the sub micro-arcsecond astrometric precision where an Earth-mass exoplanet signal lies.

As a postdoctoral fellow I plan to (i) forward model astrometric photo-center jitter of a rotating star with starspots, (ii) quantify achievable mass-precision by performing simulations of starspot debiasing and (iii) use upcoming Gaia data releases to test methods on a subset of nearby active stars. My PhD thesis in statistical signal processing and joint detection of transiting exoplanets is directly relevant in executing the proposed work on debiasing stellar jitter and characterizing the improvement in astrometric precision.

Astrometric jitter as a new lens on stars:

In a star-planet system each body orbits the mutual center of mass. By precisely measuring the star's orbital wobble, astrometry has so far been used to detect and estimate the masses of large exoplanets and secondary companion stars. Astrometry can be used to find Earth-mass planets in the habitable zones of stars within 20 pc, since unlike transit detection, where the geometric likelihood of a planet transiting falls off with semi-major axis, an exoplanets astrometric signal strength α increases with semi-major axis: $\alpha \propto \frac{M_p}{M_\star}\frac{a}{D}$, where $\frac{M_p}{M_\star}$ is the planet-to-star mass ratio, a is semi-major axis and D is distance (Shao et al., 2009). Astrometry is the path to obtaining true masses of Earth-analogs because it fits the sky plane orbit, unlike the main alternative for measuring mass, radial-velocity which yields only a minimum exoplanet mass $M_p \sin(i)$ as the orbital inclination i is unknown (Wright & Gaudi, 2012). Even so, detecting Earth-mass planets orbiting in the habitable zones of Sun-like stars requires pinpointing minuscule stellar wobbles on the order of sub-microarcseconds. At this scale, stellar surface activity, such as starspots, introduce measurable jitter in the apparent motion of the star, thus reducing sensitivity and posing a major challenge for identifying Solar-system analogs. Younger, more active or rapidly rotating stars may far exceed the Sun's 0.5 μas level of jitter at 10 pc (Shapiro et al., 2021; Nichols-Fleming & Blackman, 2019). While the sun has starspot covering fractions of the order of 0.03%, much larger starspots have been found on other stars, for example the M-dwarf TOI-3884 shows a polar spot with a possible $\approx 0.44, R_\star$ radius (Almenara et al., 2022). Starspot signatures may be strongest at bluer wavelengths where their contrast is largest (Rackham et al., 2023).

Figure 2 illustrates the potential range in starspot induced astrometric jitter noise and exoplanet signal strengths. Given this potentially large range of jitter noise, mitigating it's effect has been identified as an area of key importance to future astrometry and RV missions (Stapelfeldt & Mamajek, 2025). I will address this by using astrometric jitter noise as *information* to resolve stellar surfaces and debias starspot-induced error.

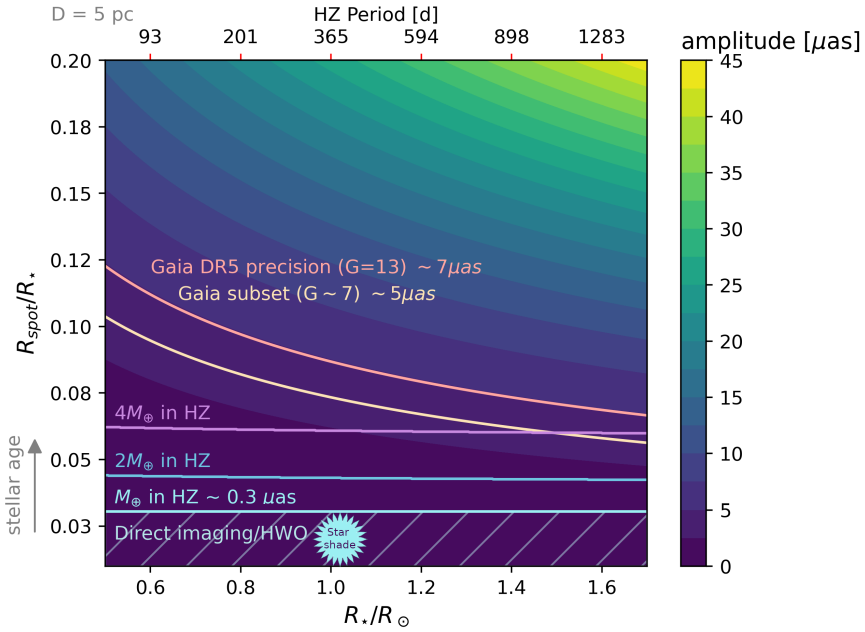

Figure 2: Astrometric jitter induced by starspots is a major source of error in precisely measuring mass. The amplitude of jitter for a single starspot is shown, varying starspot radius (y-axis) and stellar radii (x-axis), for a star at a distance of $D = 5$ pc. Part (iii) of the proposal seeks to apply starspot mapping to upcoming Gaia data. For comparison, the Gaia DR5 precision over the G-band for a $G = 13$ magnitude star is also overlaid. Below this, the Gaia precision is shown for a subset of nearby ($D < 5$ pc), young, magnetically active, stars (proposed as targets in (iii)), showing that if large starspots occur on these stars they can be detected. Future missions such as HWO aim to find and characterize Earth-mass exoplanets orbiting in the habitable zone (HZ) of sun-like stars and may rely on astrometry data to obtain complementary mass information and precursor detections. Overlaid are exoplanet signal amplitudes, where the planet is assumed to orbit in the HZ of the star. The top x-axis shows the orbital period of a planet in the HZ as it scales with stellar radius. At the Earth-mass level, relatively low levels of starspot coverage, unless corrected will prohibit the identification of true Earth analogs.

(i) A forward model from stellar surface to astrometric jitter:

Spherical harmonics provide a complete, orthonormal representation of any spherical surface and are a natural tool for describing the astrometric signal of an inclined, rotating star. By expanding the stellar surface as a linear combination of harmonics, with higher degrees capturing progressively finer structure, we can predict the rotational astrometric signature contributed by each mode individually. **My preliminary modeling reveals that astrometric signals are sensitive to a distinct set of spherical harmonic surface modes compared to photometric light curves.** Specifically, light curve primarily constrains even-degree harmonics symmetric about the equator (Cowan et al., 2013), while astrome-

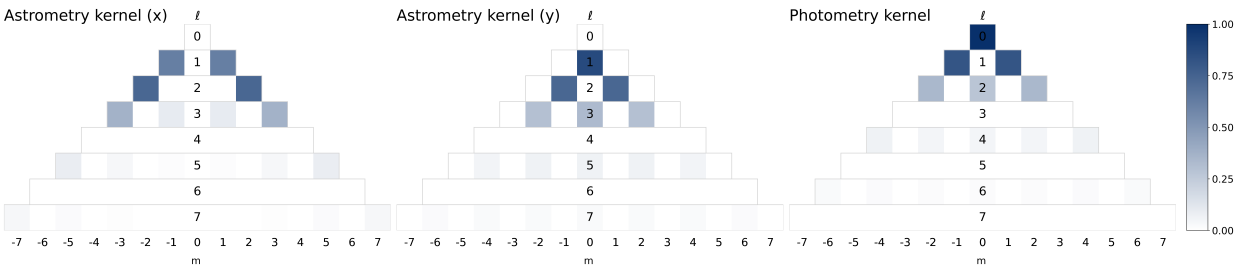

Figure 3: Visualizing the measurement kernels for astrometry and light curve photometry over the spherical harmonic basis indexed by (l, m). For a star viewed equatorially, where the kernel is 0 for the (l, m) harmonic, this harmonic term produces no measurable signal. The astrometry operator follows a pattern where even valued $l > 2$ cannot be measured, whereas the photometry operator follows the opposite pattern, odd valued $l > 2$ cannot be measured. Therefore, astrometry obtains complementary information to light curve data, and combined can attain greater reconstruction power.

try is more responsive to odd-degree modes that introduce asymmetries in the photocenter. This orthogonality is preserved for a star with an inclined rotational axis. In Figure 3, the complementary measurement spaces are shown. Stellar surface mapping is a highly degenerate problem since multiple stellar surfaces can explain the observations. **By jointly using astrometry and light curve data, the estimation sensitivity to random noise and overall identifiability of stellar surface inversion is improved, paving the way for mitigation of spot-induced noise in high-precision astrometric surveys.** Figure 4 shows example reconstructions of a simulated stellar surface, individually from astrometry and light-curve data, and jointly.

My preliminary work derives analytic expressions of astrometric jitter for a static, rotating stellar surface with an unknown inclination and finds mathematical bounds on the identifiability of the unknown surface and inclination. I propose to extend this model by incorporating time-dependent modeling. Starspots are dynamic, they may evolve, and decay on timescales that scale with spot size. Approximate relations that depend on the number of rotations have been inferred in Kepler data (Giles et al., 2017). I propose to model finite spot lifetimes and latitude-dependent drift (differential rotation) in astrometric inversion.

(ii) How does stellar surface mapping improve the precision of exoplanet mass with astrometry?

By mapping the stellar surface physically, we can more robustly identify astrometric jitter, rather than treating it as irreducible random noise. Meunier, N. & Lagrange, A.-M. (2022) show that the detection of exoplanets with longer orbital periods and in nearby stars, will be most impacted by astrometric jitter. Furthermore even for the best F-G-K candidate stars, Earth-mass uncertainties due to starspot jitter are expected to be 30% on average (Meunier, N. & Lagrange, A.-M., 2022). I propose to validate the benefit of debiasing astrometric jitter through simulated retrieval tests. By generating astrometric time series for varying levels of and spot coverage, contrasts, sizes and lifetimes and across a grid of planetary mass, orbital period, star type and inclination, I will quantify the gain in mass precision when debiasing stellar jitter.

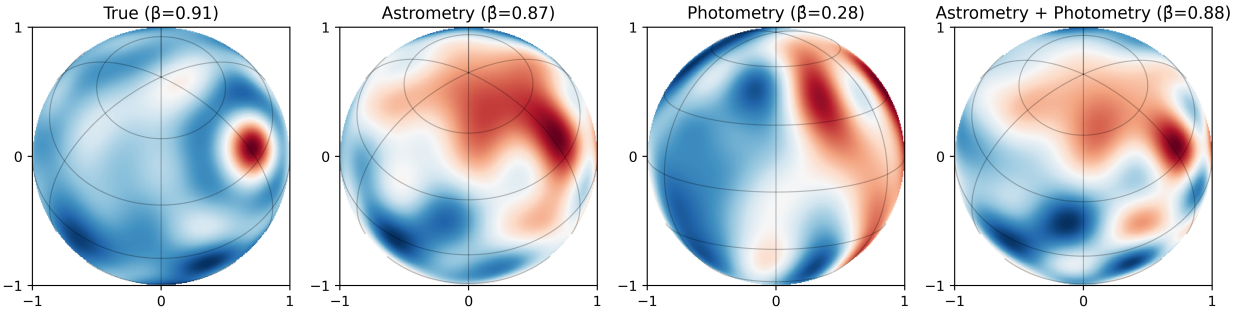

Figure 4: A ground-truth simulated surface is shown (top left) with a 8% $R_\star$ starspot, represented by a truncated spherical harmonic expansion up to $L = 10$. Reconstructions of the surface and inclination β (assumed unknown) are shown using astrometry mapping, photometry mapping, and, combined astrometry-photometry mapping. All reconstructions are generated as the regularized least-squares solution with identical priors.

(iii) Gaia data as a testing ground for astrometric inversion:

I will apply our stellar surface-mapping techniques to Gaia epoch astrometry from the forthcoming DR4 (expected late 2026), which will provide unprecedented microarcsecond-level precision over multi-year windows. A small set of nearby, active M/K dwarfs, led by AX Mic ($D \approx 3.9$ pc) and σ Dra, are candidates to show detectable astrometric jitter in Gaia's G band (330–1050 nm) (Morris et al., 2018). I will use these well-defined targets to test astrometric jitter mapping (in addition to combined astrometric light-curve mapping). For these bright $G \sim 5 - 8$ mag nearby targets, end of mission precisions in position/parallax of the order of $3 - 5\mu$as are estimated after stacking ~ 100 visits. I will develop software tools for community use to analyze Gaia data.

I will also perform astrometric mapping for a sample of target stars on the NASA ExEP's Habitable Worlds Observatory target list (Mamajek & Stapelfeldt, 2024). These are largely FGK main sequence stars within a distance of 25 pc. There are ∼541 Gaia targets within 10 pc (Reylé et al., 2022), and ∼20 overlap with NASA ExEP's ∼200-star list.

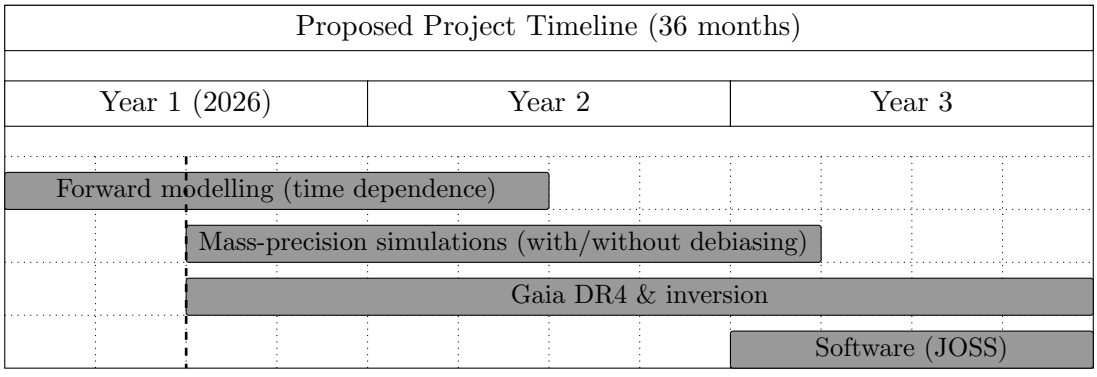

Impact:

Sub μas astrometry is key to the success of future direct-imaging missions aiming to find and characterize low-mass exoplanets. First, precise (< 10% error) mass measurements are needed to identify Earth-like atmospheres with spectral retrievals, or for

example a Nitrogen dominated Earth-like atmosphere could be confused for an O2 or CO2 dominated world (Changeat et al., 2020; Damiano et al., 2025). Second, the future Habitable Worlds Observatory (HWO) will be a NASA flagship mission and maximizing observing efficiency is critical. Precursor astrometric detections have been identified as helpful in reducing time spent on null-detections (Painter et al., 2025), which is significant given exposure times are expected to be of the order of weeks per target. The proposed work can improve the detection sensitivity to low-mass exoplanets, thereby providing more precursor exoplanet detections from astrometry. Mission design for HWO is already underway, characterizing the precision and role of astrometry is extremely timely.

Although motivated by the need to understand and mitigate stellar jitter in astrometric surveys, this work delivers a new way to map starspots and stellar surfaces, yielding new constraints on stellar magnetic activity. Because starspots additionally bias radial velocity and transmission-spectroscopy, this work will have broad reaching impact on the ability to constrain and correct their effect.

Risks:

A possible outcome in (iii) is a null detection, the main causes of a null-detection could be either insufficient sampling of a stellar rotation, excessive instrument noise or lower-than-expected spot coverage. In the latter case, a null detection would place upper limits on the level of stellar activity in these nearby stars and clarify the sensitivity floor of Gaia astrometry. Beyond Gaia data, future astrometry techniques such as diffractive-pupil astrometry have been shown in lab as a route to sub-μas precision (Guyon et al., 2011). This work will be informative for all future μas astrometry.

References

Almenara, J. M., et al. 2022, AAP, 667, L11

Changeat, Q., et al. 2020, ApJ, 896, 107

Cowan, N. B., et al. 2013, Monthly Notices of the Royal Astronomical Society, 434, 2465

Damiano, M., et al. 2025, The Astronomical Journal, 169, 97

Giles, H. A. C., et al. 2017, MNRAS, 472, 1618

Guyon, O., et al. 2011, 8151, 81510S

Mamajek, E., et al. 2024, NASA Exoplanet Exploration Program (ExEP) Mission Star List for the Habitable Worlds Observatory (2023), arXiv:2402.12414

Meunier, N., et al. 2022, AA, 659, A104

Morris, B. M., et al. 2018, MNRAS, 476, 5408

Nichols-Fleming, F., et al. 2019, Monthly Notices of the Royal Astronomical Society, 491, 2706

Painter, K. E., et al. 2025, The Astronomical Journal, 170, 147

Rackham, B. V., et al. 2023, RAS Techniques and Instruments, 2, 148

Reylé, C., et al. 2022, 218

Shao, M., et al. 2009, in astro2010: The Astronomy and Astrophysics Decadal Survey, Vol. 2010, 271

Shapiro, A. I., et al. 2021, The Astrophysical Journal, 908, 223

Stapelfeldt, K., et al. 2025, arXiv e-prints, arXiv:2507.18665

Taaki, J. S., et al. 2020, The Astronomical Journal, 159, 283

—. 2025c, The Astronomical Journal, accepted (under revision)

Taaki, J. S., et al. 2025b, The Journal of Open Source Software, 10, 7917

Taaki, J. S., et al. 2024, The Astronomical Journal, 167, 60

—. 2025a, The Astronomical Journal, 170, 14

Wright, J., et al. 2012, Planets, Stars and Stellar Systems. Volume 3: Solar and Stellar Planetary Systems, doi:10.1007/978-90-481-8818-$5_5$9